polymer

Recovery of post-yielding deformations in semicrystalline poly(ethylene-terephthalate)

A. Pegoretti*, A. Guardini, C. Migliaresi, T. Ricco

University of Trento, Department of Materials Engineering, via Mesiano 77-38050, Trento, Italy

Abstract

In this paper, aspects of the non-elastic deformation of semicrystalline poly(ethylene-terephthalate) (PET) films were studied from strain recovery and differential scanning calorimetric tests. The results show the existence of two components of non-elastic deformation, i.e. a fast-relaxing component (called anelastic) and a slow-relaxing component (usually called plastic). These strain components are both reversible and distinguished only on the basis of their different recovery times at temperatures far below the glass transition. A strain recovery master curve was built from the results of recovery tests at increasing recovery temperature. The shift-factor for the strain recovery master curve was then compared with the shift-factor for the construction of the dynamic storage modulus master curve obtained in linear regime (small strain). The aim of this comparison was to investigate the viscoelastic nature of yielding and post-yielding behavior in a semicrystalline polymer. © 1999 Elsevier Science Ltd. All rights reserved.

Keywords: Non-elastic deformation; Semicrystalline polymers; Viscoelasticity

1. Introduction

The viscoelastic nature of polymers determines a mechanical behavior strongly dependent on parameters like time, temperature and strain rate, on the basis of relationships which, in linear regime (small strain), are described by viscoelastic models and relative constitutive equations [1]. However, the viscoelastic processes involved during deformation make the determination of the yielding onset difficult. This is conventionally fixed, by following the Considére's criterion [2], as the point of relative maximum of the nominal stress–strain curve. Nevertheless, experimental evidences for amorphous glassy polymers suggest that a more attentive analysis is required [3–10]. In fact, for amorphous glassy polymers like poly(methyl-methacrylate) (PMMA), polystyrene (PS), and polycarbonate (PC), it has been proven how non-elastic deformation consists of two distinct contributes, called anelastic and plastic, which are both reversible upon heating, for strains up to 50% and more [3,4]. The distinction between the two components is made on the basis of different characteristic recovery times at temperatures below the glass transition, i.e. at $T < T_g - 20°C$ [4,6].

A molecular model for glassy polymers, first proposed by Oleynik [3], was based on a "crystal like" mechanism of plasticity. According to this model, further developed by Perez et al. [11–14], and other authors [7–9,15], at temperatures far below the glass transition, plastic strain nucleates as thermo-mechanically activated localized shear induced defects, called shear micro domains (SMD), in the presence of pre-existing quasi point defects (QPD). These are points of fluctuation in the value of local free volume of the amorphous matrix, predisposed for the easy nucleation of defects in a way that recalls the nucleation of dislocations in the crystal habit of a metal [7,9]. The borderline elastic constraint between SMDs and the undeformed matrix is the driving force for the partial strain recovery after unloading.

Due to the lack of literature information regarding the non-elastic deformations in semicrystalline polymers, the aim of the present study is to provide a contribution to the understanding of yield and post-yield behavior of a semicrystalline poly(ethylene-terephthalate) (PET) film.

2. Experimental

2.1. Materials

A commercial PET film, Mylar® (Du Pont), 52 μm in thickness, was used. Due to the biaxial orientation of the

---

* Corresponding author. Tel.: +39-0461-882413; fax: +39-0461-881977.
 E-mail address: alessandro.pegoretti@ing.unitn.it (A. Pegoretti)

Table 1
Some properties measured on the PET film

Tensile modulus E (MPa)	4500
Yield strength σ_y (MPa)	97.2[a]
Yield strain ϵ_y (%)	5.1[a]
Glass transition temperature T_g (°C)	105[b]
Melting temperature T_m (°C)	260[c]
Crystallinity content X_c (%)	36.0[c]

[a] Evaluated by the Considére's criterion.
[b] As measured with DMTA.
[c] As measured with DSC.

film, all the experiments were performed on samples obtained in the same direction, i.e. along the machine direction.

Table 1 shows the values of some properties measured on the film under the following experimental conditions.

2.2. Tensile tests

A preliminary mechanical characterization was performed by monotonic tensile tests with an Instron 4502 tensile tester, equipped with a 10 kN load cell. Tests were performed at a strain rate of 0.1 min^{-1}, on rectangular samples with dimensions $300 \times 10 \times 0.052$ mm^3 following the ASTM standard D 882-91.

2.3. Differential scanning calorimetry

A differential scanning calorimeter Mettler DSC 30 was used to detect the melting temperature, T_m, of crystalline domains and the heat released by deformed samples. The conditions for differential scanning calorimetry (DSC) measurements were as follows: specimen weight of about 20 mg; temperature range from −50 to 300°C; heating rate

of 10°C/min; nitrogen flux of 100 ml/min. The crystallinity percentage, X_c, was assessed by integrating the normalized area of the endothermal peak, and rating the heat involved to the reference value of the 100% crystalline polymer (26.9 kJ/mol) [16]. The glass transition temperature, T_g, was not detectable on the DSC curves.

2.4. Dynamic mechanical thermal analysis (DMTA)

Rectangular strips of PET film, 4 mm wide and 20 mm long, were tested by a Polymer Laboratories Ltd. (UK) MkII dynamic mechanical thermal analyzer in the tensile configuration. Tests were performed in the temperature range from −20 to 220°C, with a heating rate of 0.4°C min^{-1}, at six different frequencies, i.e. 0.3, 1, 3, 10, 30, 50 Hz. A peak to peak displacement of 64 μm was set in order to apply a small strain amplitude (in any case lower than 0.4%). The glass transition temperature T_g was evaluated as the tan δ peak temperature at a test frequency of 0.3 Hz.

2.5. Strain recovery

Residual strain of samples subjected to a preliminary strain cycle of loading, up to a certain value ϵ_0 ranging from 5 to 35%, and unloading, was evaluated on rectangular specimens, 130 mm long and 8 mm wide, cut from the original film. On the surface of the undeformed samples two marks were made with a felt tip pen and the distance, l_0, between them measured with an optical transmission microscope Leitz model Ortholux II POL-BK. The strain cycles were then performed by using an Instron machine model 4502, equipped with a 100N cell, at a constant strain rate of 0.1 min^{-1}. The distance, l, between the two marks was successively monitored after various time intervals, t_{rec}, by positioning the specimens under the microscope. Residual strain, ϵ_{res}, was then evaluated as:

$$\epsilon_{res} = \frac{l - l_0}{l_0}. \qquad (1)$$

The strain recovery tests at increasing temperatures, T_{rec}, up to 160°C, were performed on samples deformed with the Instron machine and then positioned (after a standard time of 2.5 min) in a small thermostatic chamber positioned under the microscope.

It is worth noting that no shrinkage was found on an undeformed sample kept for 2 h at the highest recovery temperature.

3. Results and discussion

3.1. Room temperature recovery tests

The characteristic shape of a stress−strain cyclic curve is reported in Fig. 1 for the case of $\epsilon_0 = 35\%$. Samples were strained up to ϵ_0, and then left to recover at room temperature, which is well below the T_g of the film. Residual strain,
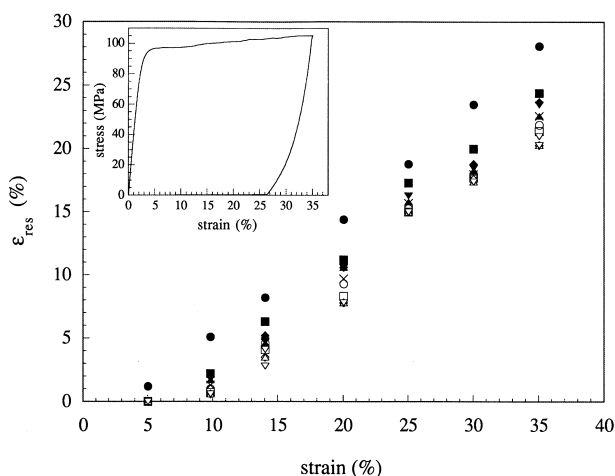

Fig. 1. Residual strain values, ϵ_{res}, as a function of the maximum strain, ϵ_0, after (●) 0 min, (■) 6 min, (◆) 15 min, (▲) 20 min, (▼) 25 min, (×) 30 min, (○) 45 min, (□) 60 min, (◇) 120 min, (△) 150 min, and (▽) 24 h from unloading, at room temperature. In the insert an example of a loading−unloading stress−strain curve up to $\epsilon_0 = 35\%$ is reported.
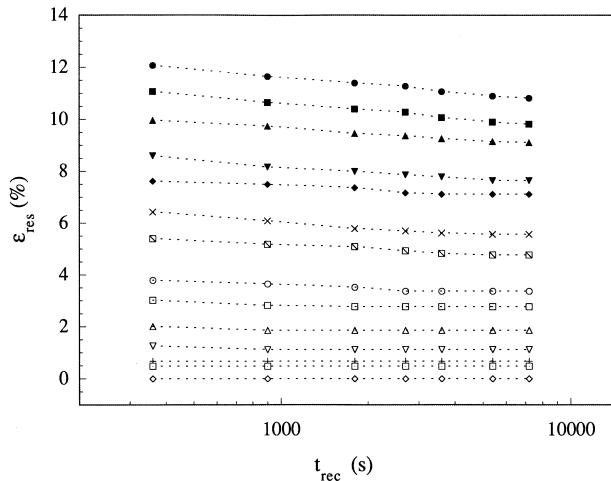
Fig. 2. Residual strain ϵ_{res}, as a function of the recovery time for samples strained up to $\epsilon_0 = 20\%$, at various recovery temperatures T_{rec}: (●) 25°C, (■) 30°C, (▲) 40°C, (▼) 60°C, (×) 70, (◩) 80°C, (○) 90°C, (□) 100°C, (△) 110°C, (▽) 120°C, (+) 140°C, (⊡) 150°C, (◇) 160°C.

measured at standard time intervals up to 24 h, are reported in Fig. 1. Strain recovery measurements during the first 6 min after unloading were not possible for the need to place the specimen under the microscope. The initial value of residual strain, i.e. ϵ_{res} at $t_{res} = 0$, is the value of strain after unloading evaluated directly on the stress–strain cyclic curves. Results reported in Fig. 1 show how, for ϵ_0 ranging from 5 to 35%, the strain recovery during unloading is followed by a further recovery which clearly depends on ϵ_0. On the basis of these results, two components of non-elastic strain can be distinguished: (i) an anelastic fast recovering component ϵ_{an}; (ii) an apparently permanent plastic component ϵ_{pl}. At this point the distinction between the two components is made exclusively on the basis of their either reversible or permanent nature at room temperature within the experimental time of 24 h. It is interesting to underline
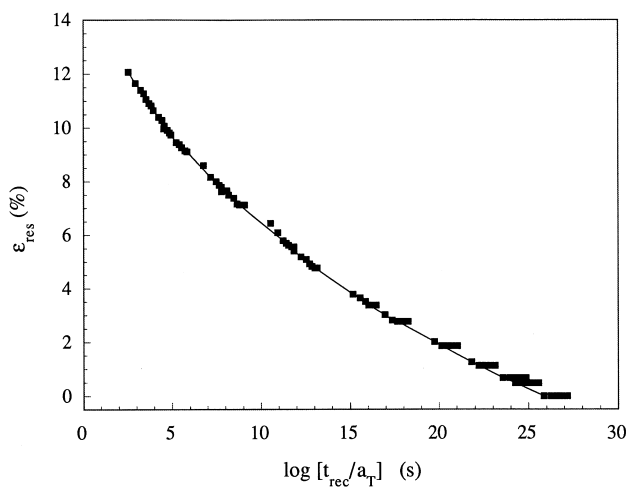

Fig. 3. Strain recovery master curve for $\epsilon_0 = 20\%$ and referred to $T_0 = 25°C$, where a_T is the appropriate shift factor.

that an initial strain of 5% is completely recovered after a time lapse of only 6 min, showing that for the material under investigation the yield point, ϵ_y, could presumably be fixed at $\epsilon_y > 5\%$.

3.2. High temperature recovery tests

As reported in Fig. 2, specimens were deformed up to a fixed strain value $\epsilon_0 = 20\%$ at room temperature, and the strain recovery observed at various recovery times, t_{rec}, at increasing recovery temperature, T_{rec}. The value of T_{rec} was increased until a complete recovery was observed within a time interval of 6 min at 160°C. Data pertinent to $T_{rec} > 25°C$ were corrected by subtracting the contribute of the thermal expansion, considering a constant value of the coefficient of linear thermal expansion equal to $1.7 \times 10^{-5} \, °C^{-1}$ [17]. The thermally activated nature of the strain recovery process is clearly evident from the fact that for any fixed t_{rec}, decreasing values of residual strain correspond to increasing values of T_{rec}. This shows how both anelastic, ϵ_{an}, and plastic, ϵ_{pl}, components are reversible and how the distinction between them is to be made not on the basis of their permanent nature, but on the basis of different recovery rates.

These results are in accordance with what has been already established for amorphous glassy polymers, beside the fact that in the case of the PET film a temperature of 45°C higher than T_g has to be reached in order to have complete recovery, whilst for amorphous polymers heating up to T_g was sufficient [4–6]. Different recovery kinetic at low temperatures indicates different activation energies for the recovery of ϵ_{an} and ϵ_{pl}, corresponding to different molecular mechanisms associated to the recovery processes.

3.3. Strain recovery master curve

A strain recovery master curve, for $\epsilon_0 = 20\%$ and referred to $T_0 = 25°C$, was built by shifting the recovery curves on a time scale, according to the time–temperature superposition principle [1]. The master curve reported in Fig. 3 shows how in a period of time of about 10^{22} years, a spontaneous complete strain recovery could eventually occur at 25°C. At this point, the derivative of residual strain with the logarithm of time was calculated, by simply evaluating the incremental ratio, $d\epsilon_{res}/(d \log(t_{rec}/a_T))$, in order to obtain a distribution of characteristic recovery times. The aim of this procedure was to distinguish the recovery of the two different components along the logarithmic recovery time scale. Nevertheless, the resulting points, reported in Fig. 4, are rather scattered, fixing a confidence band limit of 99.5% and fitting the points inside this band with a polynomial, a clear tendency emerges. The results show a spectrum of recovery times which continuously decreases, as a function of the recovery time (Fig. 4). For amorphous glassy PMMA two distinct ranges were found in the distribution [4]: a spread range at low t_{rec}, separated from a concentrated peak at very high t_{rec} by an interval where the distribution is practically nil. Physically this corresponds to the existence
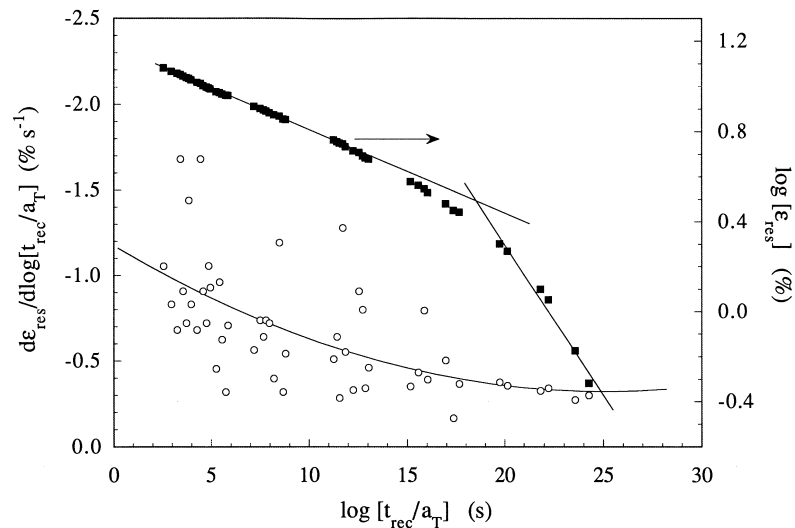
Fig. 4. Strain recovery master curve for $\epsilon_0 = 20\%$ and referred to $T_0 = 25°C$ on a double logarithmic scale, and recovery time distribution, $d\epsilon_{res}/(d\log(t_{res}/a_T))$.

of a widespread distribution of activation energies for ϵ_{an}, thus giving a wide range of relative recovery times, while the peak at high recovery times corresponds to a simultaneous recovery of ϵ_{pl} near the glass transition. In the case of the semicrystalline PET, this distinction between two ranges is absent. This is probably because of the heterogeneity introduced in the amorphous matrix by the presence of the crystalline phase, with the existence of an interphase through which there is a mobility gradient [18,19]. Mobility should be reduced near the crystals and be maximum at a distance where the presence of the crystal phase no longer interferes with the macromolecules of the amorphous phase. We could suppose that the crystals act as immobilizing agents in the amorphous matrix, thus leading to a gradient in the glass transition temperature which cause strain relaxing at various times. A tentative explanation of the observed recovery times distribution for PET could be based on the schematic reported in Fig. 5, where the recovery times

distributions for the two strain components are distinguished on a time basis.

Plotting the recovery master curve on a double logarithmic scale one can better appreciate the distinction of the two recovery kinetic regions (see Fig. 4). A transition point is evidenced by a knee in the curve and it can be tentatively fixed, at about $t_{rec} = 10^{18}$ s, as the point of intersection between the lines fitting the two regions.

3.4. DMTA results

As reported in Fig. 6, the dynamic storage modulus of the PET film was measured in a linear viscoelasticity regime, for strains lower than 0.4% at various frequencies, from 0.3 to 50 Hz, and temperatures, from −20 to 220°C. These data were subsequently rearranged by a standard time–temperature superposition principle in order to obtain the master curve reported in Fig. 7, referred to a temperature of
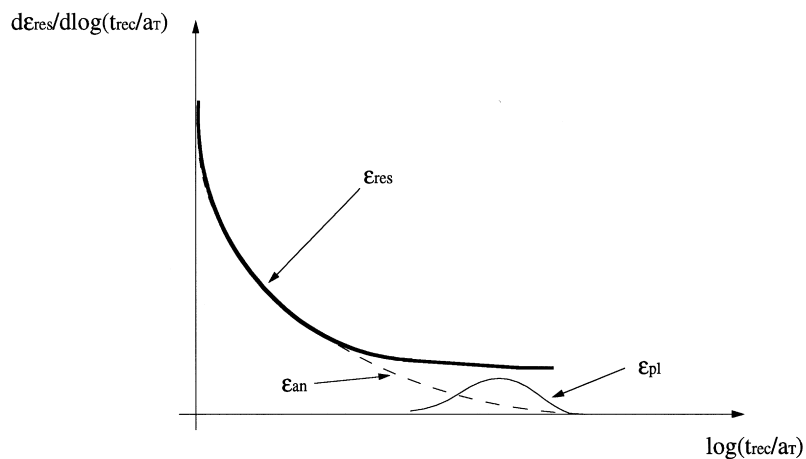

Fig. 5. Interpretation of the recovery times distribution for semicrystalline PET: an overlapping of the peaks of anelastic and plastic recovery time ranges determines an overall distribution in which a distinction between the two recovery time ranges is no longer evident.
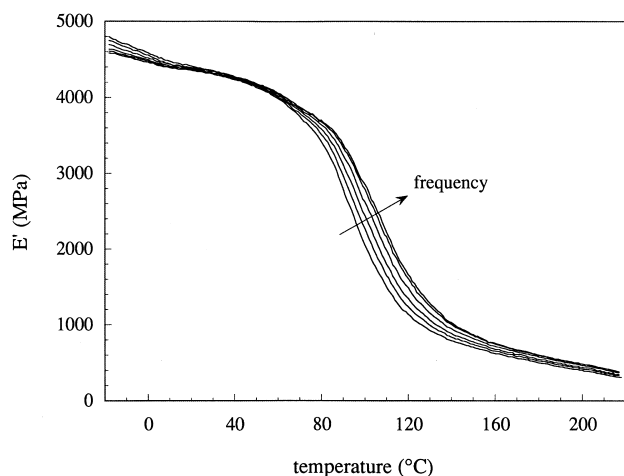
Fig. 6. Dynamic storage modulus as a function of temperature at frequencies of 0.3, 1, 3, 10, 30, 50 Hz.

Fig. 8. Comparison of shift-factors for (■) strain recovery and (●) dynamic storage modulus master curves.

98°C. The temperature dependence of the shift factors for both strain recovery and E' master curves is compared in Fig. 8. Activation energies were calculated using an Arrhenius equation for the linear parts of the curves thus obtaining 340 and 450 kJ/mol for the strain recovery and E' relaxation processes, respectively. Moreover, the glass transition temperatures, indicated by the transition point in the shift factor curves, seem to be markedly different for the two cases, being lower for the strain recovery experiments. The shift of the glass transition is a direct consequence of the presence of anelastic strains and the molecular movements involved in the growth of SMDs. These molecular motions are thought to be based on localized conformational changes in the molecular chain called elementary β-type motions [18,20], such as those that occur in the low temperature part of the α-relaxation process. These motions are active above the β-transition, which for PET is commonly around −50°C [18]. These allow the stress-induced growth of SMDs in the undeformed matrix, until
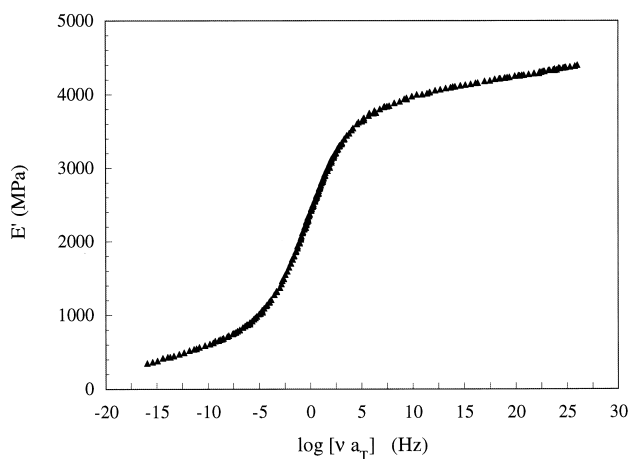
two or more SMDs borderlines meet, giving inter-molecular rearrangements, which involve α-type motions of the entire polymer chain. The combination of the two type of motions determines a broadening and shift of α-relaxation (T_g) spectrum towards lower temperatures [20]. The marked resemblance between the two shift-factor curves confirms the hypothesis on the viscoelastic nature of strain recovery mechanisms.

3.5. DSC results

DSC tests were conducted on samples deformed up to various strain levels, ϵ_0, after various recovery times, t_{rec}. The aim of this test is to evaluate the energy associated with the anelastic deformations stored in the specimens. As it is clearly evident from Fig. 9 and Table 2, the stored energy results in an exothermic peak extending from a temperature of about 60°C up to a temperature in the range from 110 to 160°C. The integral, ΔH_{EXO}, of the exothermic peak represents the energy released for the anelastic strain recovery [3,7,21–24]. As reported in Fig. 10, ΔH_{EXO} evaluated for several recovery conditions initially increases with ϵ_0, and it levels off after $\epsilon_0 = 30\%$. At a fixed strain level, the stored energy detected in the DSC measurements is decreasing as the recovery time and temperature increase. For $\epsilon_0 = 20\%$, a zero value of ΔH_{EXO} can be reached for $t_{rec} = 1$ h at $T_{rec} = 100°C$. From the strain recovery master curve (see Fig. 3) and the relative shift factors, it can be evaluated that the strain recovery at $t_{rec} = 1$ h and $T_{rec} = 100°C$ corresponds to $t_{rec} \cong 10^{18}$ s at $T_{rec} = 25°C$. This latter is also the time necessary for a complete recovery of ϵ_{an}, as we concluded analyzing the spectrum of recovery times reported in Fig. 4, according to the proposed molecular mechanisms associated to the two components. As reported in Table 3, for increasing t_{rec} and T_{rec} values, an increase of the starting temperature for the energy release can be seen,

Fig. 7. Dynamic storage modulus master curve referred to a temperature of 98°C, where ν is the frequency and a_T is the appropriate shift factor.
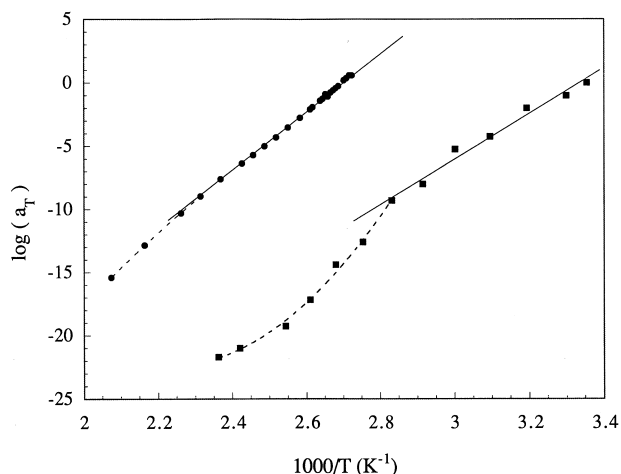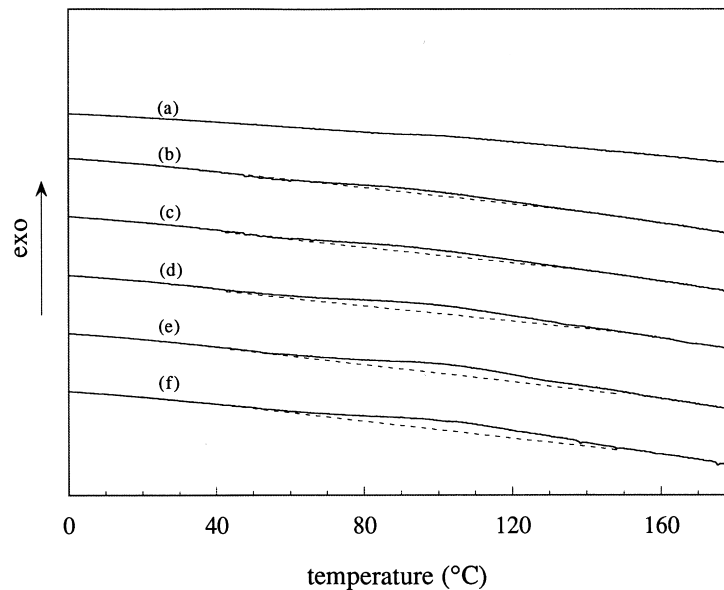
Fig. 9. Initial part of the DSC traces of PET samples previously strained at (a) $\epsilon_0 = 0\%$, (b) $\epsilon_0 = 10\%$, (c) $\epsilon_0 = 20\%$, (d) $\epsilon_0 = 30\%$, (e) $\epsilon_0 = 40\%$, (f) $\epsilon_0 = 50\%$. An exothermic peak ΔH_{EXO} is located at temperatures ranging from 60°C to a value dependent on ϵ_0.

due to the faster recovery of defects with lower activation energies.

In Fig. 11 ΔH_{EXO} values are reported for specimens deformed up to $\epsilon_0 = 20\%$ at five different deformation temperatures, T_{def}, namely 20, 40, 60, 80, and 160°C. As T_{def} increases ΔH_{EXO} decreases and for samples deformed at 160°C no energy is stored in the material. On the basis of previously discussed results, we could hypothesize a passage from a deformation mechanism typical of the glassy state, in which the primary effect is the accumulation of ϵ_{an}, to a mechanism typical of the rubbery state in which a direct nucleation of ϵ_{pl} is kinetically favourite. This behavior was explained [8,9] by considering that an increase in local free volume is associated with an increase in ϵ_{an}, with a consequent local "heating" of the material to the rubbery state where the nucleation of ϵ_{pl} becomes possible. This could also explain the shift of a_T versus lower temperatures as the effect of non-linearity in the glassy state. The specimens deformed up to $\epsilon_0 = 20\%$ at $T_{def} = 160°C$, and left to recover at 160°C, showed a really irreversible plastic deformation equal to 4.4%. At 160°C all non-elastic deformation is irreversible, i.e. disentanglement of the molecules occurs. At this point complete recovery of micro-deformation by the stretched molecules, which reassume their equilibrium tangled conformation, no longer corresponds to a recovery of macro-deformation
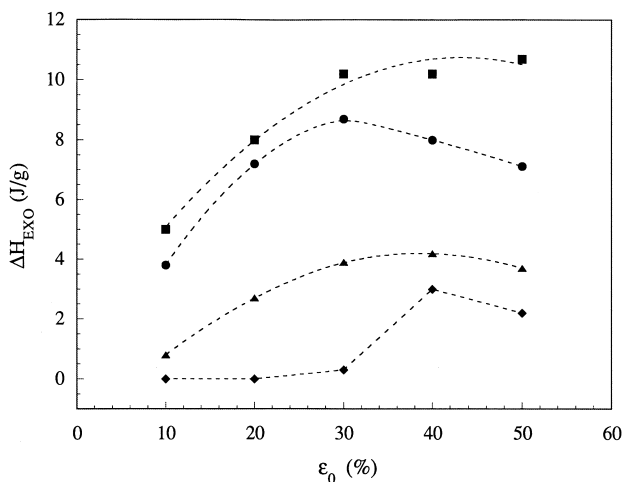

Fig. 10. Energy ΔH_{EXO}, stored in the deformed material for various levels of initial strain ϵ_0 and (■) after 5 min at $T = 25°C$, (●) after 3 months at $T = 25°C$, (▲) after 1 h at 69°C, (◆) after 1 h at 100°C (corresponding to a complete anelastic recovery).
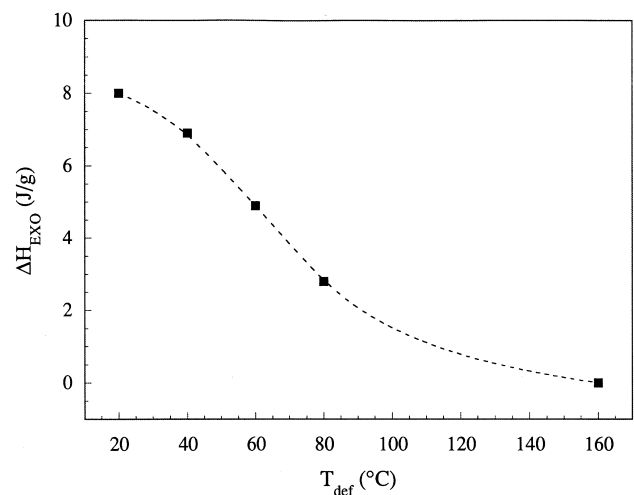

Fig. 11. Stored energy, ΔH_{EXO}, as the function of the temperature, T_{def}, at which the specimen is deformed up to $\epsilon_0 = 20\%$.

Table 2
DSC data at $t_{rec} = 5$ min and $T_{rec} = 25°C$ for specimens deformed at various ϵ_0 values

ϵ_0	Energy release starting temperature (°C)	Energy release ending temperature (°C)	Energy release peak temperature (°C)	Melting temperature (°C)	Crystallinity content (%)
10	60	117	90	260	36.3
20	60	160	97	259	35.1
30	60	160	96	260	35.8
40	60	160	100	261	35.9
50	60	160	105	260	35.9

Table 3
DSC data of specimens deformed $\epsilon_0 = 20\%$

t_{rec}	T_{rec} (°C)	ΔH_{EXO}	Starting temperature for the energy release (°C)	Melting temperature (°C)	Crystallinity content (%)
5 min	25	8	60	259	35.1
3 months	25	7.2	70	260	34.5
24 h	59	2.6	90–100	259	33.8
24 h	65	2.7	100	264	26.2
1 h	100	0.1	110–120	263	33.7

because, with the destruction of the pre-existing molecular network, the "memory" of the undeformed macro-state is cancelled. At this point a really irreversible deformation is induced.

For all the deformed specimens tested with DSC analysis, no significant changes in the area and position (see Tables 2 and 3) of the melting endothermal peak was observed, thus suggesting that deformations are limited to the amorphous regions of the material.

3.6. Strain components evaluation

Following the approach originally proposed by Quinson et al. [4] for amorphous polymers, the contribution of various components, ϵ_{el}, ϵ_{an}, ϵ_{pl}, to the total deformation

ϵ_0, can be assessed. In fact, on the basis of the information attainable from the strain recovery master curve and the relative shift factors, we can say that for an initial deformation $\epsilon_0 = 20\%$ the only residual strain component after $T_{rec} = 100°C$ for $t_{rec} = 1$ h is the irreversible plastic component. PET specimens were strained up to various levels of ϵ_0, ranging from 5 to 50%, unloaded, and successively treated in a oven at $T_{rec} = 100°C$ for $t_{rec} = 1$ h, where, as a first approximation, $\epsilon_{res} \approx \epsilon_{pl}$. At this point all strain components can be estimated from the equations below:

$$\epsilon_{an} = \epsilon_0 - \epsilon_{pl} - \epsilon_{el} \tag{2}$$

$$\epsilon_{el} = \frac{\sigma}{\widetilde{E}} \tag{3}$$
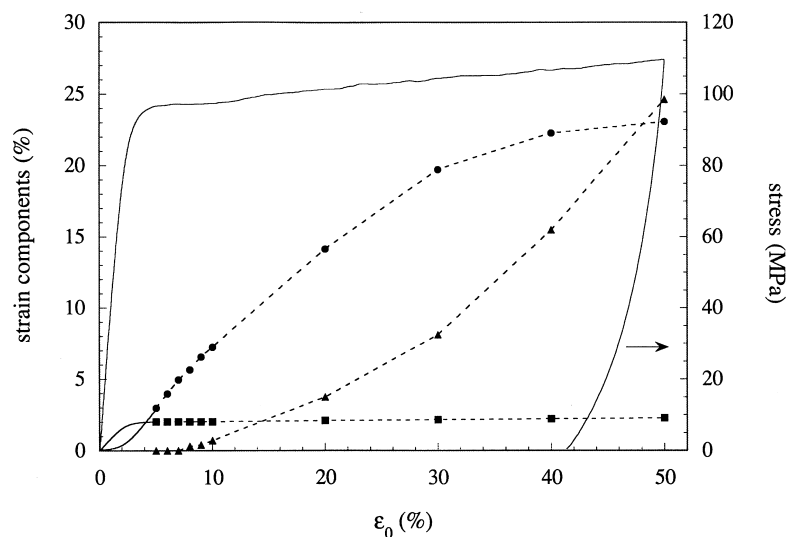
Fig. 12. Strain components as a function of the total strain ϵ_0: (■) ϵ_{el} = elastic deformation, (▲) ϵ_{pl} = plastic deformation, (●) ϵ_{an} = anelastic deformation.

where $\tilde{E}$ is the unrelaxed modulus measured at high frequencies and/or low temperatures. In the present study $\tilde{E}$ was taken as the value of the storage modulus measured at a frequency of 50 Hz and at a temperature of $-18°C$. The resulting diagram of the strain components reported in Fig. 12 clearly shows how ϵ_{an} nucleates immediately, growing up to and reaching a plateau at about $\epsilon_0 = 30–40\%$. The plastic component ϵ_{pl}, nucleates for strains higher than 7–8%, thus giving a corresponding value of the yield strain, ϵ_y, located also between 7 and 8%. According to the Considére's criterion we previously found $\epsilon_y = 5.1\%$. This discrepancy confirms the fact that the relative maximum in the stress–strain curve, conventionally thought of as macroscopic evidence of insurgence of plasticity in the material, is instead a direct effect of the anelastic component. The plastic component appears in correspondence to the onset of strain hardening, and keeps increasing while ϵ_{an} reaches a plateau. It has been shown for amorphous glassy polymers how this behavior can be well explained by the molecular model by Perez and coworkers [11–14].

4. Conclusions

Results of strain recovery tests performed on semicrystalline PET film at various strain levels and recovering temperatures, show the existence of two components of non-elastic deformation, i.e. a fast-relaxing component (anelastic) and a slow-relaxing component (plastic). These strain components are both reversible and distinguished only on the basis of their different recovery time. Strain recovery of both components is accelerated as the temperature increases. For samples deformed up to 20%, the plastic component can recover in a few minutes at a temperature about 40–50°C higher than the T_g. It is important to underline that for amorphous polymers heating up to T_g is sufficient to have a complete recovery. This difference could be explained by considering that in semicrystalline polymers a mobility gradient exists due to the interphase between crystalline domains and the amorphous matrix.

A strain recovery master curve has been constructed and the analysis of the recovery times distribution indicates that the plastic component can be recovered at times higher than 10^{18} s at room temperature. Differential scanning calorimetric analysis performed on strained samples clearly show the existence of a stored energy which is a function of the deformation level, the deformation temperature, and recovery time–temperature conditions. Finally, the contribution of various components, ϵ_{el}, ϵ_{an}, ϵ_{pl}, to the total deformation can be established.

References

[1] Ferry JD. Viscoelastic properties of polymers, New York: Wiley, 1980.
[2] Kinloch AJ, Young RJ. Fracture behaviour of polymers, London: Elsevier, 1983.
[3] Oleynik EF. In: Baer E, Moet A, editors. High performance polymers: structure, properties, composites, fibers, Munich: Hanser, 1991. p. 79.
[4] Quinson R, Perez J, Rink M, Pavan A. J Mater Sci 1996;31:4387.
[5] Quinson R, Perez J, Rink M, Pavan A. J Mater Sci 1997;32:137.
[6] David L, Quinson R, Gauthier C, Perez J. Polym Eng Sci 1997;37(10):1633.
[7] Hasan OA, Boyce MC. Polymer 1993;34(24):5085.
[8] Hasan OA, Boyce MC, Li XS, Berko SJ. Polym Sci Part B: Polym Phys 1993;31:185.
[9] Hasan OA, Boyce MC. Polym Eng Sci 1995;35(4):331.
[10] G'Sell C, ElBari H, Perez J, Cavaille JY, Johari GP. Mater Sci Eng A 1989;110:223.
[11] Mangion MBM, Cavaille JY, Perez J. Philos Mag A 1992;66:773.
[12] Perez J. Physique et mecanique des polymers amorphes, Paris: Lavoiser, 1992.
[13] Perez J, Cavaille JY, Etienne S, Fouquet F. J Phys 1980;41:C8–850.
[14] Perez J. Rev Phys Appl 1986;21:93.
[15] Bowden PB, Raha S. Philos Mag 1974;29:149.
[16] Mehta A, Gaur U, Wunderlich B. J Polym Sci Part B: Polym Phys 1978;16:289.
[17] Heffelfinger CJ, Knox KL. In: Sweeting OJ, editor. The science and technology of polymer films, 11. New York: Wiley, 1971. p. 587.
[18] McCrum NG, Read BE, Williams G. Anelastic and dielectric effects in polymeric solids, New York: Dover, 1967.
[19] Struik LCE. Physical aging in amorphous polymers and other materials, Amsterdam: Elsevier, 1978 p. 55–56.
[20] Quinson R, Perez J, Germain Y, Murraciole JM. Polymer 1995;36:743.
[21] Salamantina OB, Höhne GWH, Rudnev SN, Oleynik EF. Thermochim Acta 1994;247:1.
[22] Kung TM, Li JCM. J Mater Sci 1987;22:3620.
[23] Chang BTA, Li JCM. Polym Eng Sci 1988;28(18):1198.
[24] Adams GW, Farris RJ. Polymer 1989;30:1824.